Massaq, A., Rusinek, A., Klosak, M., Bahi, S. & Arias, A. (2019). Strain rate effect on the mechanical behavior of polyamide composites under compression loading. *Composite Structures*, vol. 214, pp. 114–122.

DOI: 10.1016/j.compstruct.2019.01.101

Strain rate effect on the mechanical behavior of polyamide composites under compression loading

Abdellah Massaq[1*], Alexis Rusinek[2], Maciej Klosak[3], Mohamed Slim Bahi[2], Angel Arias[4]

[1]Caddi Ayad University, LGECOS Laboratory, ENSA Marrakech, Avenue Abdelkrim Khattabi, Guéliz, 40000 Marrakech, Morocco

[2] Laboratory of Microstructure Studies and Mechanics of Materials, UMR-CNRS 7239, Lorraine University, 7 rue Félix Savart, BP 15082, 57073 Metz Cedex 03, France

[3]Universiapolis, Ecole Polytechnique d'Agadir, Bab Al Madina, Quartier Tilila, Agadir, Morocco

[4]University Carlos III of Madrid. Dep. Continuum Mechanics and Structural Analysis, Avda. de la Universidad 30, 28911 Leganés, Madrid, Spain

*corresponding author
e-mail addresses: a.massaq@uiz.ac.ma (A.Massaq), alexis.rusinek@univ-lorraine.fr (A. Rusinek), klosak@e-polytechnique.ma (M. Klosak), mohamed-slim.bahi@univ-lorraine.fr (M. Bahi), aariash@ing.uc3m.es (A. Arias)

Abstract: This paper presents an experimental study on the effect of strain rate on the compressive behavior of polyamide composites. Contrary to thermoset woven reinforced composites, thermoplastic woven reinforced composites have always received less interest despite its excellent damage and impact resistances. In this context, this work aims to study the behavior of fiber reinforced thermoplastic composites submitted to high strain rate in compression. The tested material is a thermoplastic composite made of armor tissue of equilibrate glass fiber and the matrix is composed of Polyamide 6 (PA6/Glass). The material is prepared with the fibers woven in 0/90 direction.

The compressive mechanical response of PA6/Glass composite was determined in the transverse and longitudinal fibers directions at quasi-static and high strain rates.The hydraulic machine and Split Hopkinson Pressure Bar experiments were conducted to determine the dynamic and quasi static compressive deformation and fracture of the PA6/Glass at strain rates from 10^{-5} s^{-1} to 1 $s^{-1}$and 100 s^{-1} to 2500 s^{-1}, respectively.

In this work, the main goals were to determine the strain rate effect on: elastic modulus, failure stress and failure energy as a function of the loading direction. The strain rate sensitivity of the failure stress level and failure energy were observed. In addition, the failure mechanism was characterized by examining the fracture surfaces using the scanning electron microscopy (SEM) method.

In quasi-static conditions of loading, the material reached its capacity due to the formation of shear bands, that concerned all three tested compression directions. In dynamics, the failure took place by

shearing followed by delamination. In case of dynamic loading in the direction perpendicular to fibers, the observations made by SEM showed that the failure of the composite had a fragile nature.

Key words: Woven composite, dynamic behaviour, dynamic fracture, Split Hopkinson Pressure Bar, failure energy, anisotropy, strain rate.

1. Introduction

Mechanical properties of a polymer composite subjected to dynamic loading strongly depend on mechanical properties of its components (fibers, matrix, interface) as well as components dimensions and their 3D distribution in the volume [1-5].

The matrix constitutes the continuum phase of the composite and its role is to link fibers together, then to transfer the mechanical loads to fibers and finally to protect fibers against any external aggression such as chemicals or moisture. The effect of the strain rate on composite matrixes was widely studied in [6, 7] where the stiffness increase was reported. Many authors showed epoxy matrixes gave a good shock resistance and high tensile resistance with high values of deformation at failure[8, 9] i.e. $\sigma_r > 69$ MPa and $\varepsilon_r > 4\%$ [8]. The best performances seem to be reached with resins based on Bisphenol A [8]. Regarding compression, high resistance is also required as this parameter is much demanded by aeronautic industry. The good compression resistance at impact must imply a high elastic modulus E. Williams [8] has shown that the matrixes with low modulus (< 3.1 GPa) give unidirectional composites with low impact resistance under compression. This is due to resin involved in the micro-buckling mechanism. On the contrary, it had little effect on tensile resistance at impact as shown by Palmer [10]. In general, Palmer demonstrated by compressing along the fibers direction that matrix properties had insignificant properties on tensile dynamic resistance. However, the tensile resistance of the matrix had an effect on the tensile resistance of the whole composite in bending and compression, for $\sigma_r \geq 55$ MPa, as well as for resistance varying between 48 MPa $\leq \sigma_r \leq$ 90 MPa. The works of Elber [11] showed that the matrix properties governed damage parameters whereas fibers properties controlled mostly the resistance to penetration. However, the fibers distribution also affects the damage mechanism. Garcia Gonzalez et al. [12] investigated the mechanical impact behavior of short carbon fiber-reinforced polyetherether-ketone (SCFR PEEK) composites using a combination of experiments and finite element simulation and summarized the penetration energy at different impact velocities. The authors concluded that the absorption energy capability of SCFR PEEK decreases drastically in comparison with unfilled PEEK. The brittleness of SCFR PEEK would limit the application of this composite in prosthetic devices employed in areas exposed to impact by accidental fall.

Fibers improve mechanical characteristics of the composite: rigidity, resistance at failure, hardness. The most popular reinforcements used for high strain rates are: glass, carbon and Kevlar®. Ayax [13] demonstrated that the total accumulated energy for unidirectional composite is higher than for a woven one. Thus, the structures with a strong anisotropy has better resistance under impact.

Harding et al. [14, 15] proved using dynamic tensile testing method that failure mechanism differed regarding whether the loading was static or dynamic. This was observed in particular for composite reinforced with glass fibers where a transition from a fragile failure to interfacial shearing (loosening

of fibers before matrix failure) was observed. This was due to the skill of glass to consummate efficiently the shock energy which makes many producers propose hybrid materials based on multi-layers of glass and carbon.

The fibers surface is often treated chemically to improve adherence with the matrix. The works of Bless [16] demonstrated that the energy threshold to perforate a composite is lower for non-treated fibers. This behaviour was also explained by Dorey [17] who showed that energy at transversal failure, which is a fundamental parameter for the impact resistance, depended on the force between fibers and matrix. He concluded the residual properties of the composite with the treated fibers are better than for the non-treated case.

Amijima et al. [18] carried out eccentric compression tests to reach the strain rates of 10^3 s^{-1} for glass/polyester unidirectional composite. The effect of the strain rates as well as of the fibers orientation (up to 45°) were considerable. However, Griffiths et al. [19] observed a difference in behaviour under static and dynamic loadings as a function of the cylindrical specimens height for unidirectional composites tested along the fibers direction.

The same specimen shape was tested in compression by Harding et al. [20] for carbon/epoxy composite. They found a slight effect of the strain rate on the Young's modulus and no effect of the specimen length on the compression resistance. However, the deformation level at failure was different for static and dynamic loadings. This change in failure mode was also observed by Bai and Harding [21]. This revealed an important effect of the friction coefficient value between the specimen and the bars faces using Split Hopkinson Pressure Bar (SHPB).

In case of compression, dynamic tests were carried out for the matrixes with different layer stacking sentences, many authors [22-24] observed the increase of the elastic modulus and failure load values when the strain rate increased.

The failure in compression is generally related to micro-buckling induced by a local misalignment of fibers. Jumahat et al. [25] explained that fibers misalignment was mostly observed in the undulated zones and generated local shearing. Gutkin at al. [26] showed this local shearing had also its origin in the decohesion between fibers and matrix. The observations at the microscopic level revealed "cups" at the fibers-matrix interfaces. Then, when compression increases, an instability appeared in the zones with strong misalignment which led to failure of fibers by bending and to propagation of kink bands [6, 26-28]. Jumahat et al. [25] observed the thickness of the kink band was approximately from 8 to 15 times the fiber diameter.

A detailed study of the process of kink bands formation was carried out by [27, 28]. They suggested a failure of fibers was the step necessary to initiate shear bands apparition. They showed fibers bent up to their break at flexion points. Finally, a folded band turned under the compression loading action to reach its final configuration. Once these conditions were reached or even overcome, the band could propagate to adjacent fibers.

Nowadays, thermoplastic composite materials experience strong growth in industries such as aerospace or automotive and this is held in many contexts. On the one hand, they are light materials which can be easily used for element production using moulding by injection method. It enables the production of complex shapes in large series and the mould has good durability. Contrary to thermosetting composites, they are recyclable. What is more, they propose remarkable mechanical and physical properties: high Young’s modulus, good shock resistance and good resistance/density ratio.

However, their heterogeneous and anisotropic structure make more difficulty in understanding and characterizing their damage under dynamic loading.

Among thermoplastic composite materials, those with glass fibers and Polyamide (PA) demonstrate a large potential in engineering applications. Major applications of PA6s are in automotive parts where they are used as electrical connectors and light-duty gears. Glass reinforced resins are used for engine fans, radiator heaters, brake-fluid reservoir, valve covers and hydraulic hoses. They are also used as hammer handles, gears and sprockets, bushing and cams. Electrical applications include wiring devices, plugs, connectors, power-tool housing, washers and small appliances. They are also used in ski boards, roller skater, bicycle wheels and fishing lines. Biaxially oriented PA film is extremely tough and is used for meat and cheese packaging, cook-in-bags and vacuum-fill pouches.

Dally et Carillo [29] highlighted why among thermoplastic composite materials, those with glass fibers and polyamide (nylon) matrix are of interest. The fatigue tests showed that for glass fibers composite the polyamide presented better performances in terms of resistance and life duration than polyethylene or polystyrene. This is mainly due to higher cohesive energy for polyamide [30]. The polyamide 6 (PA6) has excellent properties such as hydrogen bone in molecular chains of the polyamide which makes it one of the major engineering and high performance plastics [31].

However, the understanding of the mechanical behaviour of these materials under dynamic loading conditions is limited due to the associated technical hitches at high strain rates. This can be improved by using Split Hopkinson Pressure Bar (SHPB) [32] which remains one of the most popular techniques for dynamic tests. The dynamic compression tests are more suitable than tensile ones for fragile materials and polymer composites because of fixation problems. Then, a heterogeneity and diversity in fiber orientation make composite materials more demanding when it comes to tensile tests more than to compression ones.

Most of the high strain-rate characterization studies are focused towards the thermosetting composites such as epoxy and polyester matrices which are reinforced mainly with carbon and glass fibers [33-37]. A number of studies were performed in recent years on the strain rate effect on the mechanical properties of thermoplastic composites [38-43]. Few works [44-46] were reported on the dynamic compressive response of polyamide composites. Strain-rate dependency is one of the material behaviors of fiber reinforced composites being focused on because many primary structural applications involve exposure to impact and crash loads. Ploeckl et al.[47] studied the strain-rate effect on the longitudinal compressive strength of UD carbon-fiber-reinforced PA6 and showed 60% strength increase at the same strain level. Elmarakbi et all. [48] investigated the crashworthiness response for a hierarchical modelling of hybrid composite material consisting of short-glass fibers reinforced graphene platelets (GPL) polyamide PA6 matrix. They showed the contribution of GPL as significant in terms of specific energy absorption SEA.

As mentioned, the effect of strain rate on the mechanical properties of composite materials has been studied since several years. However, there is still a need to get more reliable data for engineering design. Additionally, the failure mechanism under different strain rates needs to be clarified. The objective of this study is to determine the effect of strain rate on the mechanical behaviour of the woven glass-fiber-reinforced Polyamide PA6 composite. The dynamic test results are compared to the quasi-static values. The procedure proposed in [49] is applied to treat stress-strain curves obtained through dynamic compression tests in order to eliminate errors related essentially to friction, inertia or

wave dispersion. Finally, imperfections of the materials with occurring damage under dynamic loading are observed and analyzed.

2. Sample preparation and properties

The material used is a thermoplastic composite made of armour tissue of equilibrate glass fiber and a matrix composed of Polyamide 6 (PA6/Glass composite). It is fabricated using a double belt press (Fig. 1).The glass fibers have an average diameter of 10 μm and define 50 % of the total volume. The weave pattern is shown, Fig. 2.

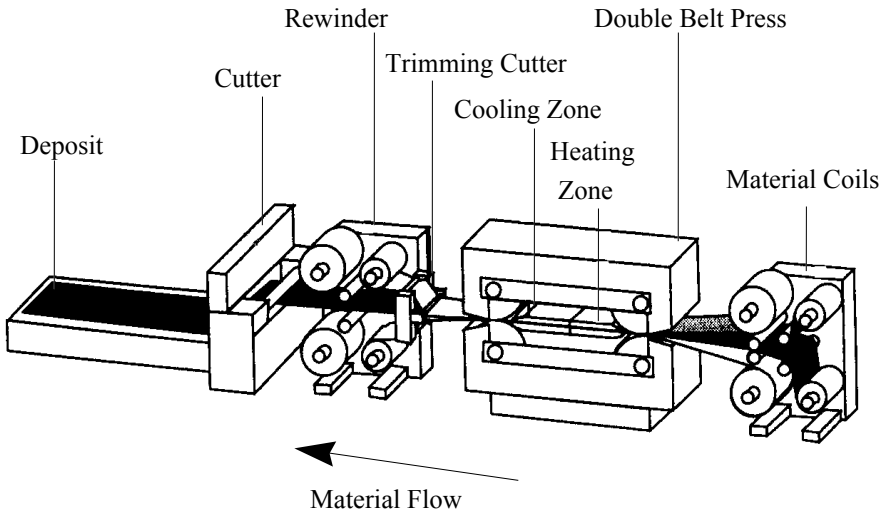

Figure 1: Double belt press machine used for composite design [50]

The tests were carried out on cylindrical specimens, loaded in compression along the three directions: L1, L2 (L being the longitudinal direction to the fiber) and T (transversal direction to the fiber), see Fig. 2. In order to minimize errors related to friction or those due to radial inertia, the specimens were relatively short with a ratio length over diameter close to 1.0.

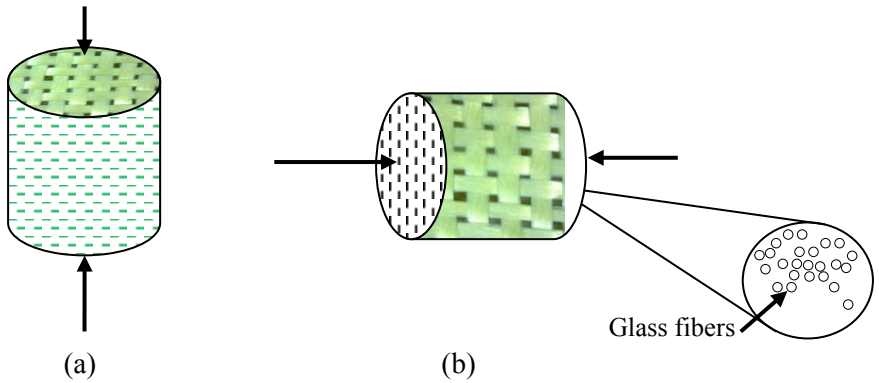

Figure 2: Description of the loading directions and of the weave pattern, a) transversal direction to the fiber, b) longitudinal direction to the fiber

In order to explain the strain rate influence on the tested material, the effect of the loading velocity on the mechanical response of the PA6/Glass composite in different compression directions will be presented in the next part. Then, the analysis of the surfaces on which the impact was applied will help to explain the failure mechanism in static and dynamic loading conditions.

3. Methodology of compression tests

A complete study for a wide range of strain rates was performed under compression using a hydraulic machine (Zwick) which is available to deliver a maximum force of 100 kN and a displacement of 300 mm. Using this device, the strain rate varies between 10^{-5} s^{-1} to 1 s^{-1}.

In order to perform dynamic compression, Split Hopkinson Pressure Bar (SHPB) system is used. A short specimen is placed between two long elastic bars. The loading is performed thanks to a projectile impacting the input part, Fig. 3. The well known SHPB technique is discussed for example in [51].

Using SHPB, the maximum strain rate is close to $5 \cdot 10^3$ 1/s

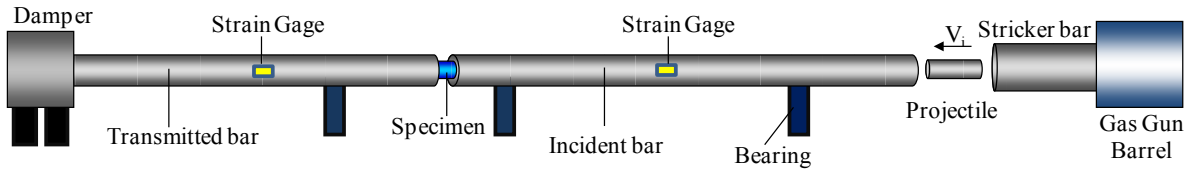

Figure 3: Hopkinson pressure bar technique (SHPS) for compression tests with displacement gages

Dynamic compression tests are frequently used to characterize material behaviour at high strain rates, mainly for metals or some polymers. However, problems arise when the material used is composed of a thermoplastic matrix. Some disadvantages can be listed, one example is the wave reflection at the interface fiber-matrix which induces a phenomenon of the wave dispersion in the material.

For a complete definition of the mechanical properties of the composite during compression tests a procedure developed and described in [49] was applied. It eliminates the errors essentially due to the problems related directly to testing conditions such as friction, inertia or wave dispersion. This procedure takes into account friction effects as well as the wave dispersion in the vicinity of bar-specimen contact zone.

4. Test results

4.1 Compressive strength at strain rates from about 10^{-5} s^{-1} to 1 s^{-1}

The force-displacement recorded allow to calculate the stress-strain curves. The curves are presented in Fig.4 for three compression directions: L1, L2 (L is the longitudinal direction of the fibers) and T (T is the transversal direction to the fiber). It can be deducted from the curves that for the three compression directions the material behaves in a semi-fragile way. On the one hand for small strains, these curves present elastic linear behaviour. This linear behaviour strongly varies as a function of strain rate in the T compression direction. On the other hand, the linear part is followed by a non-linear one and this is when the strain rate sensibility is remarkable for the L compression direction. This observation can be explained by the beginning of the material deformation.

This fragile behaviour is more important for the cases when compression is applied along the direction of fibers which is due to the poor resistance at failure.

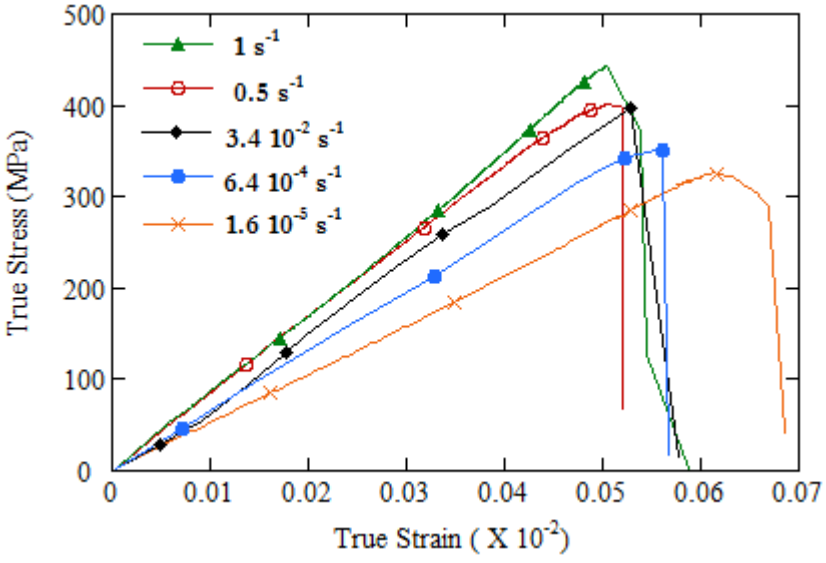

(a)

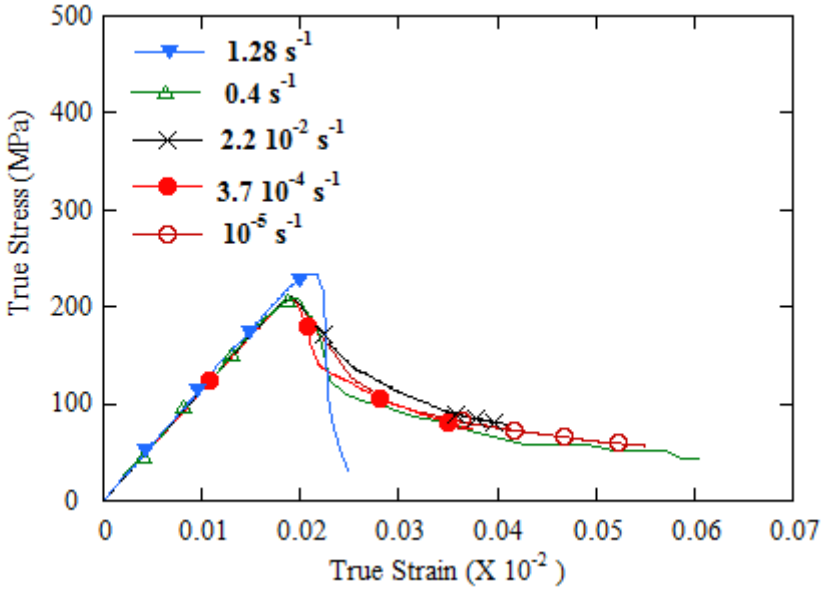

(b)

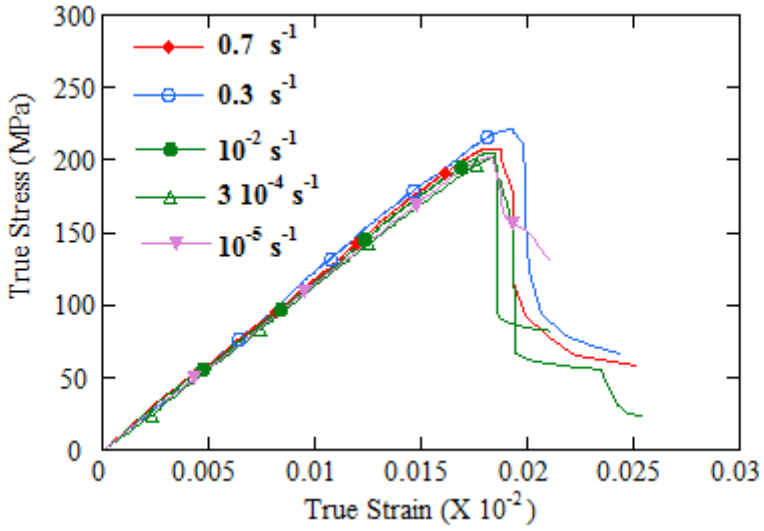

(c)

Figure 4: Stress-strain curves for quasi-static compression tests (a) transversal compression direction T, (b) longitudinal compression directions L1, (c) longitudinal compression directions L2

4.2. Compressive strength at high strain rates from about 100 s^{-1} to 2500 s^{-1}

The problem of dispersion could be corrected by a factor from the solution of the equation of frequencies related to an infinite cylinder [52], obtained by Pochammer et Chree. The same approach was used by [49] in which the wave was decomposed by the Fast Fourier Transform (FFT). Then, a correction of dephasage was proceeded thanks to the solution of the equation of frequency. Thus, the signal was reconstituted by Fourier's transform (FFT^{-1}).

When the incident wave $\varepsilon_I(t)$, reflected wave $\varepsilon_R(t)$ and transmitted wave $\varepsilon_T(t)$ are measured along the bar, it is possible to describe the strain, stress curves on time. However, before using the elastic waves ε_{wave}, a FFT treatment is performed to consider the Pochammer-Chree effect [53, 54] inducing elastic waves dispersion, which were applied to the case of longitudinal waves in cylindrical bar by Bancroft [55].

$$\varepsilon_{dispersion}(t) = FFT^{-1}\left[e^{-i\Delta x\left[\xi(\omega)-\frac{\omega}{c_0}\right]}FFT(\varepsilon_{wave}(t))\right] \quad (1)$$

where $\varepsilon_{wave}(t)$ is the elastic wave measured along the bars on time.

The results are reported in the following picture, Fig. 5. It is observed that the correction allows to reduce some frequency inducing a smooth of the original signal.

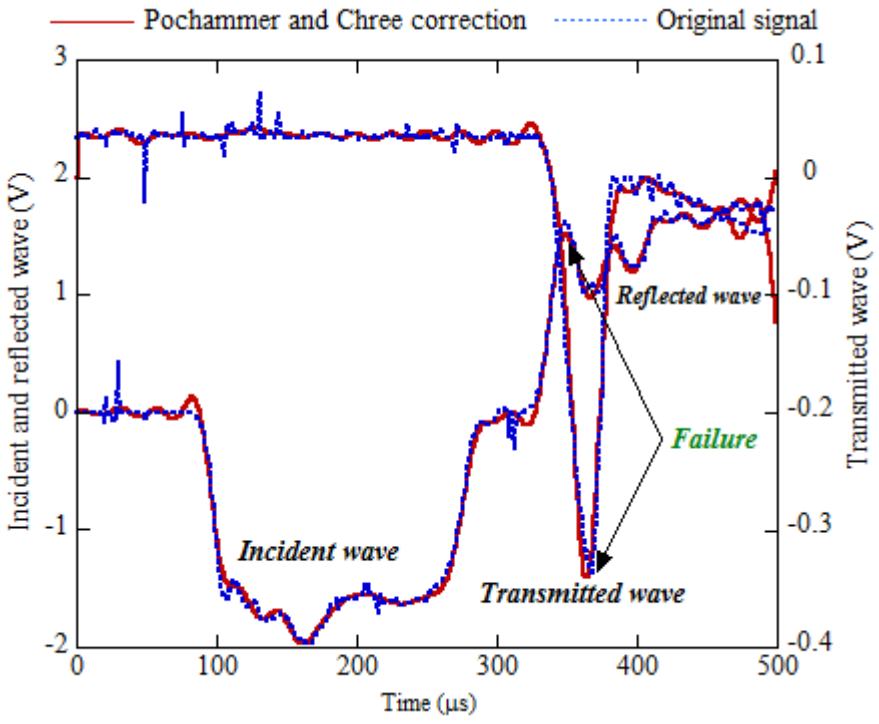

Fig. 5. Comparison between the original waves and after dispersion correction

Using the previous measurements, the following equality corresponding to a force equilibrium may be used, Eq. 2.

$$\varepsilon_I(t) = \varepsilon_R(t) + \varepsilon_T(t) \tag{2}$$

Moreover, the stress, strain and strain rate may be defined thank to the elastic waves and assuming a one-dimensional stress wave theory [56]. Thus, the strain rate is defined as follows, Eq. 3.

$$\dot{\varepsilon}_s(t) = 2\frac{c_o}{l_o}\varepsilon_R(t) \tag{3}$$

where l_0 is the initial length of the specimen and c_0 is the celerity of the elastic wave in a bar.

Using the previous equation, Eq. 3 and integrating it over time, the strain may be calculated, Eq. 4.

$$\varepsilon_s(t) = 2\frac{c_o}{l_o}\int_o^t \varepsilon_R(\xi)\,d\xi \tag{4}$$

Finally, the average stress applied to the specimen is defined, Eq. 5.

$$\sigma_s(t) = \frac{E_b A_b}{2 A_s}[\varepsilon_I(t) + \varepsilon_R(t) + \varepsilon_T(t)] \tag{5}$$

where A_s is the initial cross-section of the specimen, E_b is the Young's modulus of bars, A_b is the cross-section of the bars. The stress defined Eq. 5, may be reduced to Eq. 6, assuming a forces equilibrium, Eq. 2.

$$\sigma_s(t) = E_b\left(\frac{A_b}{A_s}\right)\varepsilon_T(t) \tag{6}$$

The difficulty in the SHPB system consists essentially in the elastic waves transport. Deformations are measured experimentally at the surface of the bar. Theoretically, they should correspond to the axial displacement of the complete cross-section of the bar. This could only be possible if the propagation of the wave inside the bar is unidimensional, i.e. the displacements of all points of a given cross-section are uniform. However, during the impact of the projectile into the incident bar, the generated wave is of a certain irregularity in its beginning phase, this is principally due to geometric irregularities at the interface bar-projectile.

In order to provide a more reliable description of the material behaviour in dynamic conditions, it is essential to take account of errors related to phenomena which occur systematically during the tests. One of the main artefacts changing the material behaviour in terms of stress level is related to the friction effect on the bars-specimen interface. In addition, inertia is also acting on the measurement but this effect is smaller in comparison with the friction effect [57].

Therefore, the stress defined for the material behaviour $\sigma(t)$ using Split Hopkinson Pressure Bar (SHPB) is defined as follows, Eq. 7:

$$\sigma(t) = \tilde{\sigma}_{measured}(t) + \Delta\tilde{\sigma}_{\mu}(t) \tag{7}$$

The term corresponding to the overstress state related to friction without inertia effect may be calculated using the model proposed by Klepaczko-Malinowski [58] and detailed in [57].

$$\Delta\tilde{\sigma}_{\mu}(t) = \frac{\mu.\phi_S}{3.l_S}\tilde{\sigma}_{measured}(t) \tag{8}$$

Where μ is the friction coefficient, l_S is the length of the specimen and ϕ_S is the diameter of the specimen. Therefore, if a lubricant is used to reduce the friction effect, the stress calculated $\sigma(t)$ and based on the waves corresponds to the stress level imposed on the specimen $\Delta\tilde{\sigma}_{\mu}(t) \to 0$. In order to understand more precisely the PA6/Glass composite behaviour in dynamic compression, and in particular the failure mechanism, a series of tests have been carried out. The main interest was paid to the evolution of the resistance in compression and the energy at failure as a function of the strain rate. The large range of strain rates was studied, namely from 100 s^{-1} to 2500 s^{-1}.

For each test condition, three specimens were tested. Figure 6 represents a summary of the stress-strain curves of the PA6/Glass composite, loaded parallel and perpendicularly to fibers.

The shape of stress-strain curves depends essentially on the strain rate and fibers direction. It is deduced from these curves that the elastic modulus of the composite in L compression direction is superior to that in T compression direction. The sensibility to strain rate of the maximum stresses is more important for T direction than for L direction. Many authors [59-61] postulated this augmentation of stress flow in function of strain rate due to secondary processes at molecules level. The thermoplastic matrix ensures the transfer of the mechanical loading on the fibers and delay the failure of it in contrary to the thermosetting matrices. The use of a polyamide thermoplastic matrix makes it possible and improve the resistance to cracks propagation. In addition, this kind of matrix allows to absorb a large amounts of energy through it molecular structure and allows a high energy dissipation by sliding of the molecular chains relative to each other. Indeed, it gives them a larger failure deformation and toughness.

In the configuration L, the fibers work directly in compression what explains small deformations in this direction, mostly because of the elevated elastic modulus value. The resistance at failure of the material is higher in T direction than in L direction. Once the failure level is reached, the stress level drops dramatically. The material failure is of the fragile nature in both directions of loading.

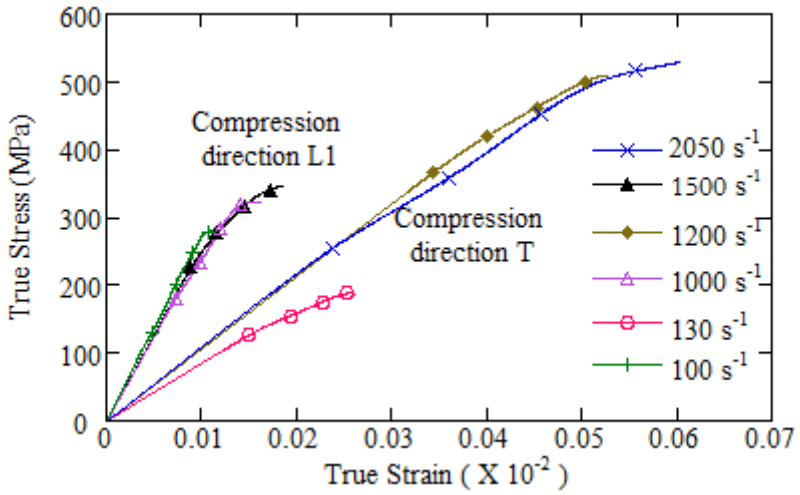

(a)

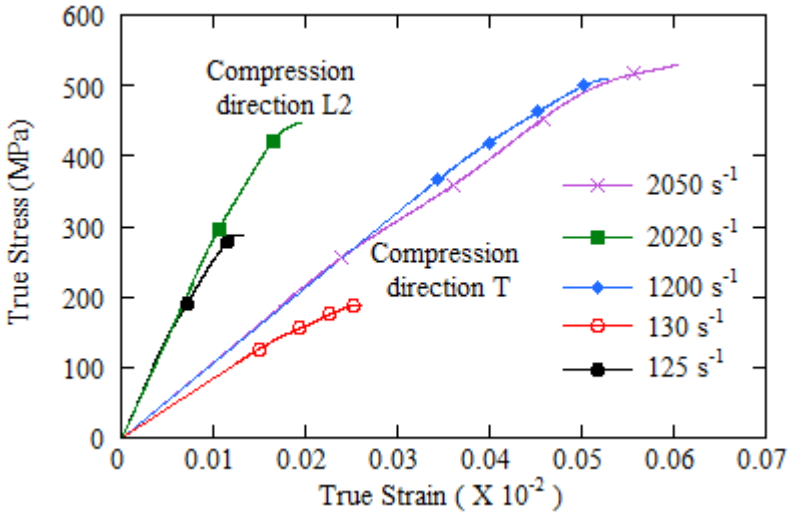

(b)

Figure 6 : Comparison of stress-strain curves (a) compression directions L1 and T, (b) compression directions L2 and T

During the dynamic tests, the absence of plastic deformation of the PA6/glass composite is found. The thermomechanical coupling is then neglected, because the rise of the temperature within the composite material during the deformation is very slow.

5. Discussion

5.1. Influence of strain rate

The exploitation of the quasi-static tests results allowed to determine a value of the failure stress in compression for the PA6/Glass composite. In parallel, for the dynamic regime, the strain rate effect on the failure stress value was revealed. Figures 7, 8 and 9 present the influence of the strain rate on the failure stress level for the three compression directions L1, L2 and T. These results demonstrate a positive sensibility of failure stresses to strain rates in compression.

In the compression directions L1 and L2, the failure stresses remain insensible to strain rates in quasi-static domain. On the contrary, in the dynamic domain, the strain rate effect takes a predominant role in changing the failure stress for PA6/Glass composite. The results obtained for the compression directions L1 and L2 are different from those recorded for the compression direction T. In the latter case, the failure stress represent an almost linear function of the strain rate. A considerable strain rate sensitivity is reported in both domains: quasi-static and dynamic.

In the T direction where the matrix is acting more than the fibres, the material behaviour is reporting a viscous behaviour. The viscous behaviour is related to the strain rate sensitivity of the polyamide matrix. It is typically observed for semi-crystalline polymers [62]. In quasi-static conditions and due to the long loading time (few mintues) applied to the specimen in comparison with dynamic loading (few ms to μs), the relaxation phenomenon is easier and therefore more important.

The modelling of the curve presented in Fig. 9 is made using the least squares method which permits to calculate the sensitivity coefficients of the failure stress to strain rate (quasi-static and dynamic). The coefficients are calculated in the way to minimize differences with experimental results.

The stresses evolve according to the following equation:

$$\sigma_r\left(\dot{\varepsilon}\right)=\sigma_{r_0}+\beta\log\left(\dot{\varepsilon}/\dot{\varepsilon}_0\right) \tag{9}$$

For $\dot{\varepsilon}=1\,s^{-1}$, it corresponds to the failure stress in quasi-static conditions along the T compression direction: $\sigma_{r_0}=435\,MPa$. This is close to the experimental value, Fig. 4, with $\sigma_{r_0}^{\exp}\approx 442\,MPa$. The parameter β represents the strain rate sensibility coefficient of the failure stress value, β = 25 MPa.

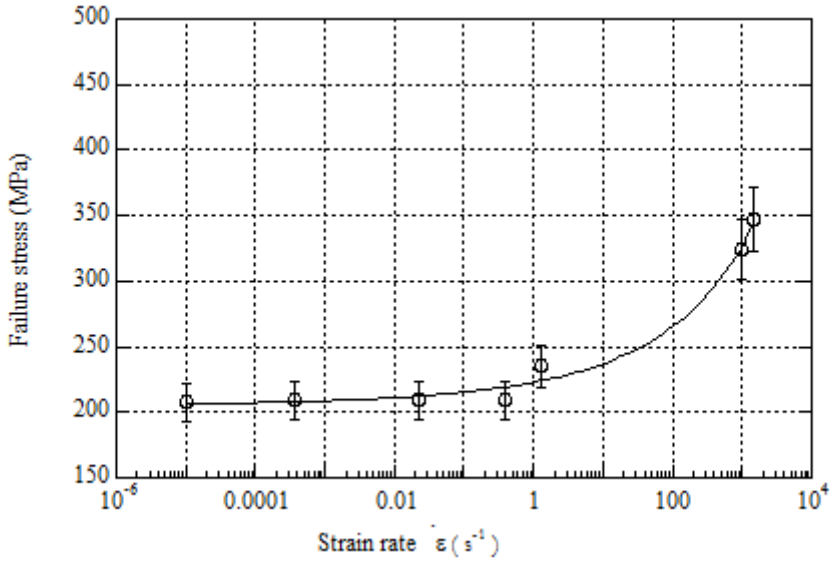

Figure 7: Influence of strain rate on failure stress value; compression direction L1

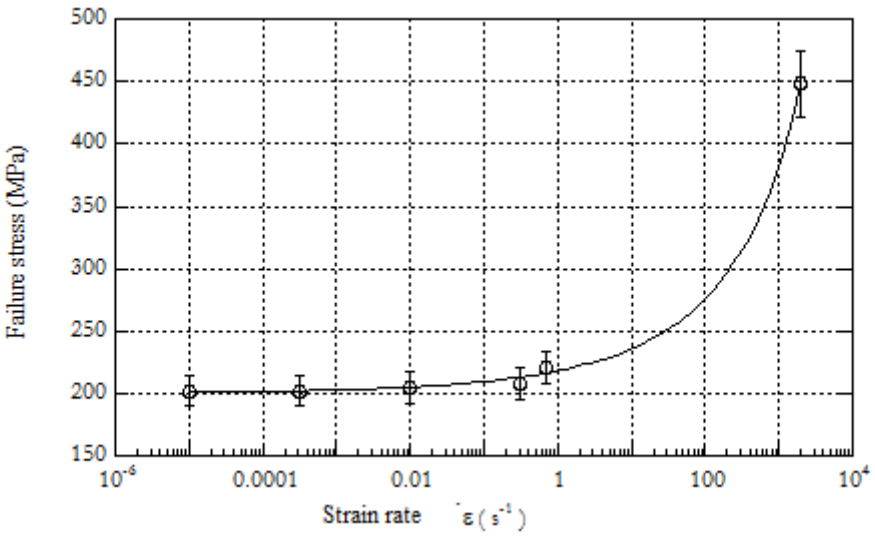

Figure 8: Influence of strain rate on failure stress value; compression direction L2

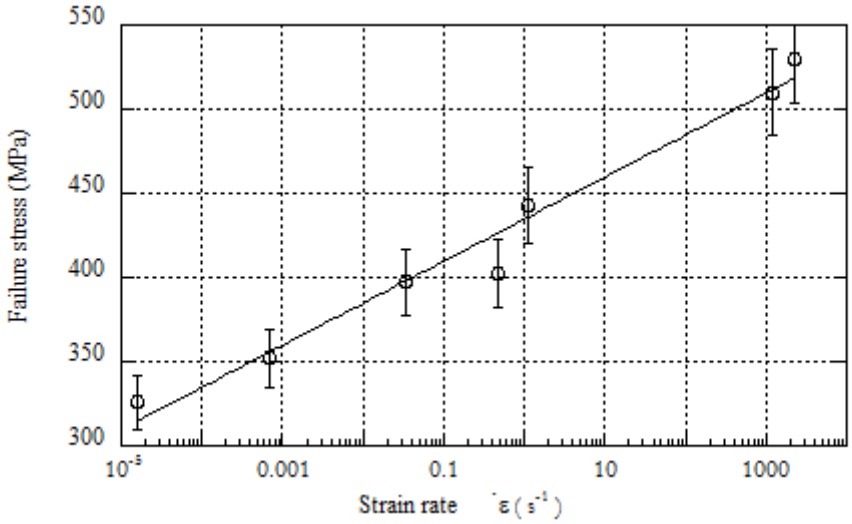

Figure 9: Influence of strain rate on failure stress value; compression direction T

Figure 10 illustrates the sensibility of stresses to the strain rate effect of the PA6/Glass composite for a given deformation level of 0,01 and for three compression directions (L1, L2 et T). The same algorithm of the least squares method is used to generate the curves. The linear correlation of this curve is given by the following equation:

$$\sigma_{\varepsilon=0.01}\left(\dot{\varepsilon}\right)=\sigma_0+\alpha\log\left(\dot{\varepsilon}/\dot{\varepsilon}_0\right) \tag{10}$$

For $\dot{\varepsilon}=1\ s^{-1}$, it represents the stress level for a strain level of 0.01 under quasi-static conditions, α is the strain rate sensitivity coefficient at deformation level of 0.01, α = 6 MPa. For the T compression direction σ_0 = 82 MPa, the stress value is higher for the L directions, σ_0 = 115 MPa. Comparing α to β, Eq. 9, it can be noticed that the strain rate sensibility is more important for the stress level close to failure.

In case of the T compression direction, the strain rate sensitivity is moderated in the whole range of strain rates. In case of the L compression directions, the strain rate sensibility is more important, but only above the strain rate level of 10^2 s^{-1}.

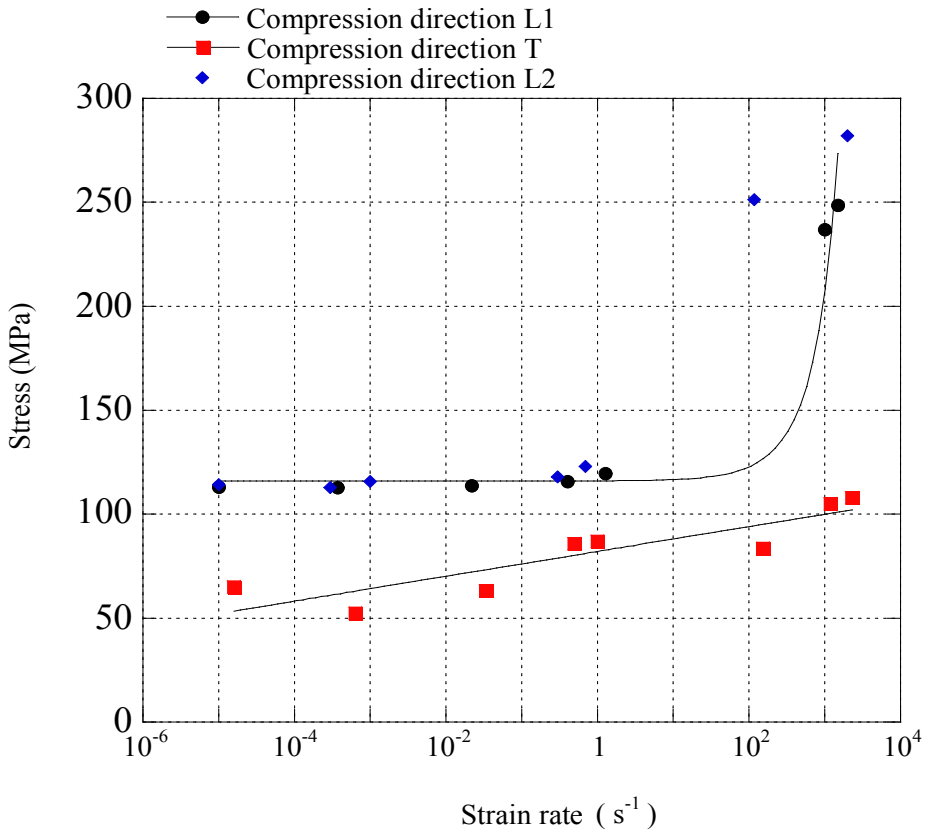

Figure 10: Stress as a function of strain rate; strain level of 0.01

Figure 10 reveals the existence of three ranges of the strain rate effect, two of them being for L direction and one for T direction. The first one corresponds to quasi-static loadings, the failure stress being little affected by this parameter, rather non sensitive at all. The second range corresponds to high speed loading for which a strong strain rate effect is observed. In this last zone, the mechanism of the viscous drag is predominant and the composite behaves in a quasi-viscous manner. Both concern the L1 and L2 directions. The third range is described by a quasi-logarithmic impact of the strain rates on the failure stresses - such behaviour is recorded for the T direction.

The failure test is also intended to measure a ratio of the restitution energy which is defined as the energy absorbed by the specimen during shock. The total energy at failure $W_{failure}$ is defined as follow:

$$W_{failure} = S_0 \; l_0 \int_0^{\varepsilon_r} \sigma(\varepsilon) \, d\varepsilon \qquad (11)$$

where S_0 and l_0 are respectively the cross-section and initial length of the specimen and ε_r is the deformation at failure.

The variation of the energy at failure value of the PA6/Glass composite is a function of the strain rate for all three compression directions L1, L2 and T and is reported in Fig. 11. This energy at failure value increases with the impact velocity. This increase is more important for the direction T than for directions parallel to fibers distribution (L1 and L2).

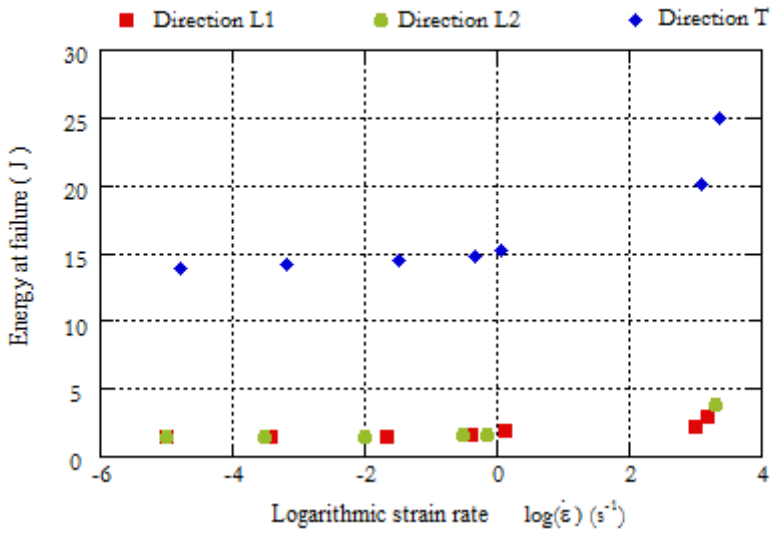

Figure 11: Influence of strain rate on energy at failure

During the dynamic test, the absence of the plastic deformation was observed. It may lead to conclusion that for the PA6/Glass composite a thermomechanical coupling can be neglected, i.e. the increase of temperature in the material as well as material deformation are very low.

5.2. Failure modes for PA6/Glass composite

In quasi-static compression: in order to describe qualitatively the damage and failure mechanisms, the post-test observations of specimen faces were made. For three compression directions, the material perishes due to shearing. Figures 12 and 13 illustrate the state of the specimens smashed in quasi-statics. The failure mode is the shearing for both longitudinal and transversal compression directions. The shearing makes the specimen separate into several parts. The failure surface is inclined at ≈ 54° and starts at the corner of the specimen (Figure 12-b).

The mechanism of shearing in composites has not been well explained yet. Some authors, for example R. Effendi [56], proposed to attribute it to plastic instability of the matrix and to geometrical initial imperfections of fibers (fiber undulations, misalignment). Under the compression load, these imperfections amplify and the zones of stress concentrations appear in the matrix. This process leads to an instability and provokes shearing bands formation which accelerate the final failure of composite.

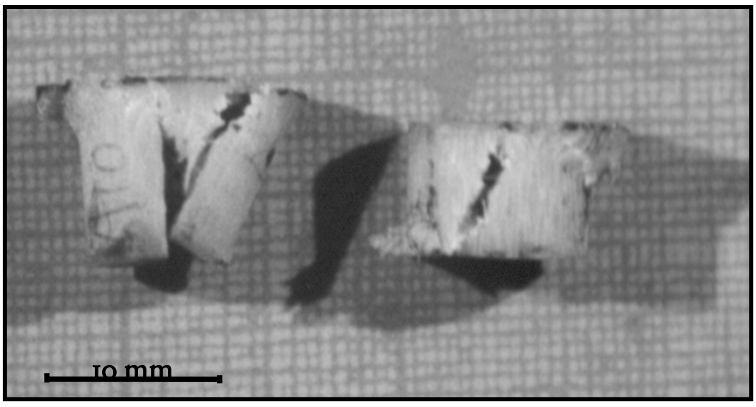

(a)

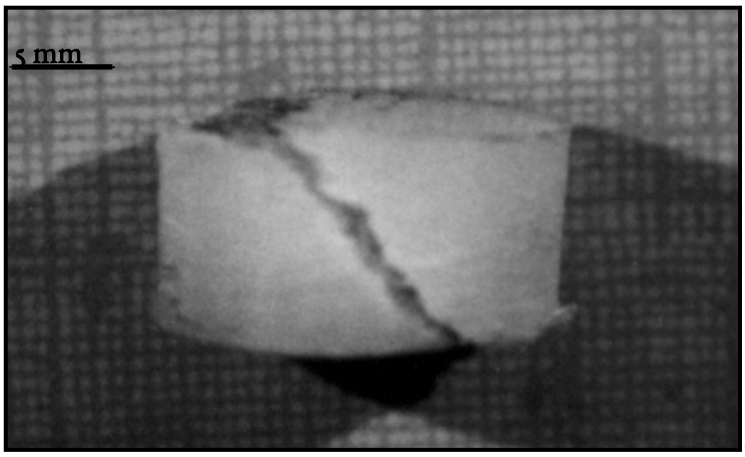

(b)

Figure 12: Shearing in specimens in quasi-static loading, a) compression directions L, b) compression direction T

Figure 13: Double band of folding, compression directions L

When the dynamic compression in the transversal direction T is considered, a failure appears after the shearing zone is created. On the contrary, for the compression longitudinal directions L, the failure is produced through the shearing of fibers followed by the delamination and finally to decomposition into several tranches. Sometimes the state of failure is quasi-general, this is due to the peeling off of fibers and to the crack propagation in the matrix. The observations made by using the scanning electron microscope of the failure surfaces confirmed the described aspects of the fragile failure of the material tested under dynamic conditions (Fig. 14).

In the direction T, this is due to the fragilization of the matrix related to the diminution of the mobility of molecular chains. Figure 14 presents the SEM micrograph obtained for the directions L. Pictures of the surface of fragile failure with transversal cracking is shown, the phenomenon is related to poor adherence between matrix and fibers. This poor adherence depends on the fiber-matrix interface, fibers length and thickness. If improved, it can considerably enhance fiber protection against shock. Figure 14-c clearly shows the fiber pull-out with a considerable length encountered during the dynamic compression.

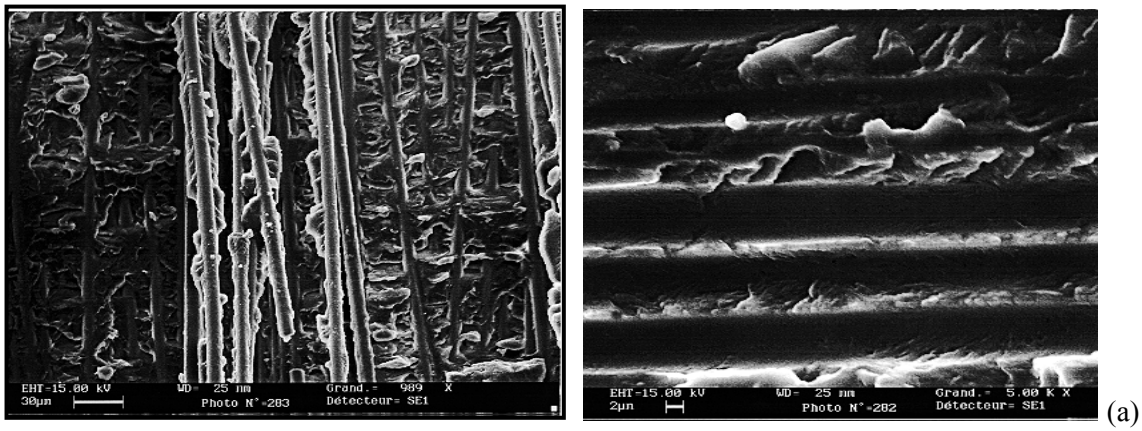

(a)

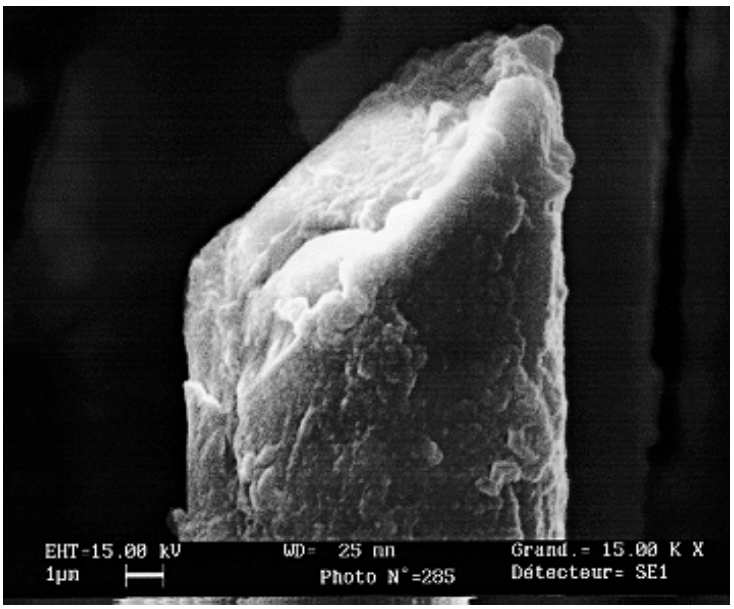

(b)

Figure 14: Rupture of a ply of glass fibers, a) the matrix after decohesion of fibers at the failure level, b) fiber pull-out

6. Conclusions

The use of different experimental techniques to cover quasi-static and dynamic behaviour allowed to determine composite characteristics of the composite in the large range of strain rates from 10^{-5} s^{-1} to 2500 s^{-1}. Experimental data revealed an important strain rate sensibility on: the elastic modulus, failure stress and failure energy. This was observed especially for the strain rates superior to 1 s^{-1}. This strain rate sensibility is also dependent on the compression direction (longitudinal or transversal).

Another observation was the fact that the material presented little resistance to shock, being fragile in all three directions in which it was solicited. Concerning a thermomechanical coupling, a very small temperature increase in specimens was registered. This was due to a brittle material behaviour which did not attribute enough time for heating before failure.

The experimental results also provided data about deformation at failure values as well as failure mode for PA6/Glass composite. In regime quasi-statique, it is shown that the composite failed by shear banding along the diagonal axis. The microscopic observations on the failed samples have proved that the composite failed by the decohesion between fibers and matrix and fibers pull out mechanisms. These observations confirmed the fragile failure of the polyamide composite under dynamic conditions. It was also confirmed that the failure is a direct consequence of the damage which precedes it. This damage phase is particularly interesting in order to understand a failure mechanism of PA6/Glass composites.

REFERENCES

[1] Ibrahim SM, Almusallam TH, Al-Salloum YA, Abadel AA, Abbas H. Strain Rate Dependent Behavior and Modeling for Compression Response of Hybrid Fiber Reinforced Concrete. Latin American Journal of Solids and Structures 2016;13:1695-1715.

[2] Chiu P-H, Vecchio KS, Nesterenko VF. Dynamic compressive strength and mechanism of failure of Al-W fiber composite tubes with ordered mesostructure. International Journal of Impact Engineering 2017;100:1-6.

[3] Kern WT, Kim W, Argento A, Lee E, Mielewski DF. Mechanical behavior of microcellular, natural fiber reinforced composites at various strain rates and temperatures. Polymer Testing 2014;37:148-155.

[4] Yang F, Ma H, Jing L, Zhao L, Wang Z. Dynamic compressive and splitting tensile tests on mortar using split Hopkinson pressure bar technique. Latin American Journal of Solids and Structures 2015;12:730-746.

[5] Yoo D-Y, Banthia N, Kang S-T, Yoon Y-S. Effect of fiber orientation on the rate-dependent flexural behavior of ultra-high-performance fiber-reinforced concrete. Composite Structures 2016;157:62-70.

[6] Sun CT. Testing and Modeling Rate Dependent Properties of Polymeric Composites Using Off-axis Specimens. CompTest 2003.

[7] Fan JT, Weerheijm J, Sluys JL.Compressive response of multiple-particles-polymer systems at various strain rates. Polymer 2013;91:62-73.

[8] Williams JG, Rhodes MD. Effect of resin an impact damage tolerance of graphite/epoxy laminates composite materials. Testing and Design, 6th Conf. ASTM STP 787, Ed. I. M. DANIEL; 1982:450.

[9] Disalvo GDM, Lee SM. Fracture tough composites. The effect of toughened matrices on the mechanical performance of carbon fiber reinforced laminates. 14th SAMPE Tech. Conf.; 1982:491.

[10] Palmer RJ. Investigation of the effect of resin material on the impact damage to graphite-epoxy composites. NASA-CR-165677;1981:1.

[11] Elber W. Failure mechanics in low velocity impact on thin composite plates. NASA Tech Paper; 1983:2152.

[12] García-Gonzalez D, Rodriguez-Millán M, Rusinek A, Arias A. Low temperature effect on the impact energy absorption capability of PEEK composites. Composite Structures 2015;134:440-449.

[13] Ayax E. Caractérisation expérimentales et modélisation du comportement d'une plaque composite tissée en règime balistique. Thèse de l'ENSAM de Bordeaux; 1993.

[14] Harding J, Welsh LW. A tensile testing technique for fibre-reinforced composites at impact rates of strain. J. of Mat. Sci. 1983;18(6):1810-1826.

[15] Saka K, Harding J. The deformation fracture of hybrid reinforced composites under tensile impact. ICCM6 London; 1987.

[16] Bless SJ, Hartman DR. Ballistic penetration of S-2 glass laminates. Proc. 21st Int SAMPE Conf.; 1989:852.

[17] Dorey G. Relationship between impact resistance and fracture toughness in advanced composite materials, Effectof Service Environment on Composite Materials. AGARD CP 288; 1980.

[18] Amijima S,Fuju T. Compression strength and fracture characteristics of fiber composites under impact loading. Material Technology, Serie N° 2, Ed. Carlos J.Hidalgo; 1970:398.

[19] Griffiths LJ, Martin DJ. A study of the dynamic behaviour of a carbon-fiber composites using the split Hopkinson pressure bar. J. Phys-D.1974;7:2329.

[20] Harding J, Li LY, Saka K, Taylor MEC. Characterization of the impact strength of woven carbon fiber/epoxy laminates. Inst. Phys. Conf. Ser., Oxford 1989;102:403.

[21] Bai Y. Harding J. Fracture initiation in glass-reinforced plastics under impact compression. Proc. Int. Conf. on Structural Impact and Crashworthiness, Imperial College, London 1984;2:482.

[22] Zeltmann SE, Prakash KA, Doddamani M, Gupta N. Prediction of modulus at various strain rates from dynamic mechanical analysis data for polymer matrix composites. Composites Part B 2017;120:27-34.

[23] Asprone D, Cadoni E,Prota A, Manfredi G. Strain-Rate Sensitivity of a Pultruded E-Glass/Polyester Composite. Journal of Composites for Construction 2009;13(6):558-564.

[24] Bragov AM,Lomunov AK. Mechanical properties of some polymers and composites at strain rates of 1000/s. Journal de Physique IV, Colloque C8, supplément au journal de Physique III, 1994;4:337.

[25] Jumahat A, Soutis C, Jones FR, Hodzic A. Fracture mechanisms and failure analysis of carbon fibre/toughened epoxy composites subjected to compressive loading. Composite Structures 2019;92(2):295-305.

[26] Gutkin R, Green C, Vangrattanachai S, Pinho S, Robinson P, Curtis P. On acoustic emission for failure investigation in CFRP: Pattern recognitionand peak frequency analyses. Mechanical Systems and Signal Processing 2011;25(4):1393-1407.

[27] Steiff PS. A model for kinking in fiber composites - I: Fiber breakage via microbuckling. International Journal of Solids and Structures 1990;26:549.

[28] Steiff PS. A model for kinking in fiber composites - II: Kink band formation. International Journal of Solids and Structures 1990;26:563.

[29] Dally JM,Carillo DH. Fatigue Behavior of Glass-Fiber Fortified Thermoplastics.Polymer Engineering and Science 1969;9(16):434.

[30] Guérin B. Polyamides PA. Techniques de l'ingénieur; 1994.

[31] Hamida F, Akhbara S, Ku Halim KH. Mechanical and Thermal Properties of Polyamide 6/HDPE-gMAH/High Density Polyethylene. Procedia Engineering 2013;68:418-424.

[32] Pierron F. Beyond Hopkinson's bar. Philos. Trans. R. Soc., London 2014;A372.

[33] Li X, Yan Y, Guo L, Xu C. Effect of strain rate on the mechanical properties of carbon/epoxycomposites under quasi-static and dynamic loadings. Polymer Testing 2016;52:254-264.

[34] Naresh K, Shankar K, Velmurugan R. Reliability analysis of tensile strengths using Weibull distribution in glass/epoxy and carbon/epoxy composites. Composites Part B: Engineering 2018;133:129-144.

[35] Shokrieh MM, Rezvani S, Mosalmani R. Mechanical behavior of polyester polymer concrete under low strain rate loading conditions. Polymer Testing 2017;63:596-604.

[36] Gurusideswar S, Velmurugan R, Gupta N. Study of rate dependent behavior of glass/epoxy composites with nanofillers using non-contact strain measurement. International Journal of Impact Engineering 2017;110:324-337.

[37] Shokrieh MM, Rezvani S, Mosalmani R. Mechanical behavior of polyester polymer concrete under low strain rate loading conditions. Polymer Testing 2017;63:596-604.

[38] Kapoor R, Pangeni L, Bandaru AK, Ahmad S, Bhatnagar N. High strain rate compression response of woven Kevlar reinforcedpolypropylene composites. Composites Part B 2016;89:374-382.

[39] Carrillo JG, Gamboa RA, Flores-Johnson EA, Gonzalez-Chi PI. Ballistic performance of thermoplastic composite laminates made from aramid woven fabric and polypropylene matrix.Polym. Test 2012;31:512-519.

[40] Garcia-González D., S. Garzon-Hernández, A. Arias. A new constitutive model for polymeric matrices: Application to biomedical materials. Composites Part B: Engineering 2018;139(15):117-129.

[41] Alcock B, Cabrera NO, Barkoula NM, Wang Z, Peijs T. The effect of temperature and strain rate on the impact performance of recyclable all-polypropylene composites. Compos. Part B 2008;39(3):537-547.

[42] Barany T, Izer A, Karger-Kocsis J. Impact resistance of all-polypropylene composites composed of alpha and beta modifications.Polym. Test. 2009;28(2):176-182.

[43] Martin A, Othman R, Rozycki P. Experimental investigation of quasi-static and intermediate strain rate behaviour of polypropylene glass fibre (PPGF) woven composite, Plastics, Rubber and Composites.Maney Publishing 2015;44(1):1-10.

[44] Qian X, Wang H, Zhang D, Wen G. High strain rate out-of-plane compression properties of aramid fabric reinforced polyamide composite. Polymer Testing 2016;53:314-322.

[45] Ploeckl M, Kuhn P, Koerber H. Characterization of unidirectional carbon fiber reinforced polyamide-6 thermoplastic composite under longitudinal compression loading at high strain rate. EPJ Web of Conferences 2015;94:01041.

[46] Bondy M, Altenhof W. Low velocity impact testing of direct/in line compounded carbon fibre/polyamide-6 long fibre thermoplastic. International Journal of Impact Engineering 2018;111:66-76.

[47] Ploeckl M, Kuhn P, Grosser J, Wolfahtr M, Koerber H. A dynamic test methodology for analyzing the strain-rate effect on the longitudinal compressive behavior of fiber-reinforced composites. Composite Structures 2017;180:429-438.

[48] Elmarakbi A, Azotia W, Serry M. Multiscale modelling of hybrid glass fibres reinforced graphene platelets polyamide PA6 matrix composites for crashworthiness applications. Applied Materials Today 2017;6:1–8.

[49] Massaq A, Rusinek A, Klósak M, Abed F, El Mansori M. A study of friction between composite-steel surfaces at high impact velocities. Tribology International2016;102:38-43.

[50] Wong J. Processing of High Performance Thermoplastic Composites. Spring Semester 2017, 131-5048-00L Manufacturing of Polymer Composites; 2017.

[51] Massaq A, Rusinek A, Klósak M. Method for determination of the dynamic elastic modulus for composite materials. Engineering Transactions 2013;61(4):301-315.

[52] Klepaczko JR. An experimental technique for shear testing at high and very high strain rates. The case of mild steel. Int. J. Impact. Engng. 1994;15(1):25-39.

[53] Pochhammer L. Ueber die Fortpflanzungsgeschwindigkeiten kleiner Schwingungen in einem unbegrenzten isotropen Kreiscylinder. Journal für die reine und angewandte Mathematik 1876;81:324-336.

[54] Chree C. The equations of an isotropic elastic solid in polar and cylindricalco-ordinates their solution and application. Transactions of the Cambridge Philosophical Society 1889;14:250.

[55] Bancroft D. The velocity of longitudinal waves in cylindrical bars. Physical Review 1941;59:588-593.

[56] Alves M, Karagiozova D, Micheli GB, Calle MAG. Limiting the influence of friction on the split Hopkinson pressure bar tests by using a ring specimen. Int. J. Impact. Eng. 2012;49:130-141.

[57] Jankowiak T, Rusinek A, Lodygowski T, ‘Validation of the Klepaczko–Malinowski model for friction correction and recommendations on Split Hopkinson Pressure Bar. Finite Elements in Analysis and Design 2011;47(10):1191-1208.

[58] Klepaczko JR, Malinowski Z. Dynamic Frictional Effects as Measured from the Split Hopkinson Pressure Bar. In Kawata K and Shioiri J. Eds.: High Velocity Deformation of Solids. Springer-Verlag, Berlin. 1978:403-416.

[59] Rana D, Sauvant V, Halary JL. Molecular analysis of yielding in pure and antiplasticizedepoxyamine thermosets. Journal of Materials Science 2002;37:5267-5274.

[60] Richeton J, Ahzi S, Daridon L, Rémond Y. A formulation of the cooperative model for the yield stress of amorphous polymers for a wide range of strain rates and temperatures. Polymer 2005;46:6035-6043.

[61] Richeton J. Modeling and validation of the finite strain response of amorphous polymers for a wide range of temperature and strain rate. Ph. D dissertation, Université Louis Pasteur Strasbourg I; 2005.

[62] Mouhmid B, Imad A, Benseddiq S, Benmedkhène N, Maazouz A. A study of themechanical behaviour of a glass fibre reinforced polyamide 6,6: Experimental investigation. Polymer Testing 2006;25:544-552.62